LINEAR STABILITY ANALYSIS OF STRATIFIED TWO-PHASE FLOW IN A PLANE CHANNEL USING NUMERICAL SIMULATIONS

Deibi E. García[1], deibi.g.c@gmail.com
Daniel Rodríguez[1,2], dani@mec.uff.br
Igor Braga de Paula[1], igordepaula@puc-rio.br
Angela O. Nieckele[1], nieckele@puc-rio.br
[1]Mechanical Engineering Department, Pontifícia Universidade Católica do Rio de Janeiro (PUC-Rio), Rio de Janeiro, RJ, 22451-900, Brazil
[2]Laboratory of Theoretical and Applied Mechanics (LMTA), Graduate Program in Mechanical Engineering (PGMEC), Department of Mechanical Engineering, Universidade Federal Fluminense, Niterói, RJ 24210-240, Brazil

Abstract. *Linear stability theory has been used for decades for prediction of transition from stratified two-phase flow to other different flow regimes like slug, roll-waves or annular. The results from stability analysis of two phase flows in horizontal pipelines are often useful for a wide variety of industrial application in areas such as oil production, nuclear, chemical and many others. A major part of the works devoted to address the problem of instability in two phase flows consider that once the flow becomes unstable to growth of infinitesimal disturbances, there is a change in the flow pattern. A method extensively used in the literature to estimate whether disturbances would growth or decay is the linear temporal stability analisys. Although spatial instability analysis is more closely related to practical applications, it has not been sistematically used for the problem at hand. This work presents a study of the linear stability of pressure-driven plane channel flow with two immiscible fluids with different viscosity and density at low Reynolds number, both in the temporal and spatial frameworks. As opposed to similar approaches based on the one-dimensional two-fluids model, which impose uniform velocity profiles for each phase, at the present work a two-dimensional formulation is employed with the VOF (volume of fluid) model to capture the interface. The conservation equations are solved with the finite volume method with a time and space second order schemes. Good agreement is obtained with results from a linear stability analysis analogous to the Orr–Sommerfeld equations for the dominant wavelengths, frequencies and phase velocities.*

Keywords*: Linear stability, Two-phase flow, VOF Method, Interfacial waves, Orr–Sommerfeld approach*

1. INTRODUCTION

Hydrodynamic stability analysis of flows in channels, pipes and flat plates has been used extensively in literature to study the conditions required for a stable flow to become of an unstable type, thus predicting flow pattern transitions. The complexity of two-phase flows is significantly greater than the single-phase case, as they involve continuously deformable interfaces. Depending on the flow conditions, the fluids can be arranged in the form of some widely known patterns in the fluids transport industry such as stratified, slug, roll-waves, or annular flow, among others.

In the framework of two-phase flows in horizontal pipelines, different approaches were found in the literature to address the problem. For example, in the study of slug formation, early one-dimensional approach based on the two-fluid model (Ishii and Hibiki, 2011), indicate good prediction of some results when are compared with experimental data, but not for others (Eduardo et al., 2015; Salhi et al., 2010; Guo et al., 2002; Barnea and Taitel, 1993; Lin and Hanratty, 1986; Taitel and Dukler, 1976). Most of these practical models are highly restrictive to assume, among other things, that an unstable small-amplitude long wave would grow into a slug, driven by some kind of Kelvin–Helmholtz instability (Valluri et al., 2008). On the other hand, more rigorous models based on the Orr-Sommerfeld equations applied to two-phase flow (Valluri et al., 2008; Kuru et al., 1995; Yiantsios and Higgins, 1988), have less restriction and therefore can report better results when compared against early models. Such studies result from improved capabilities of present computers over the last decades as well as from recent developments in numerical techniques. This enable the extension, of less restrict stability analysis to two-phase flow problems (Rodríguez, 2015).

Numerical simulation is another method used to predict behaviour of the two-separated phases. Recently, this technique has been used to validate results of the Orr-Sommerfeld analysis (Valluri et al., 2010; Valluri et al., 2008; Cao et al., 2004). For plane parallel flows (Couette and Poiseuille) different techniques have been employed to model the evolution of a very small interfacial perturbation in two-phase flow, such as level set (Valluri et al., 2008), front-tracking method (Cao et al., 2004) and diffuse-interface method (Valluri et al., 2010). Another surface-tracking technique very attractive, although little used in this area, is the VOF (Volume of Fluid) method, which main characteristic is to guarantee mass conservation. This work is focus in this approach.

Commonly, in case of parallel flows, a study of the local modal linear stability, describes the evolution of modes (waves) which might grow or decay in time, space or both, indicating whether the flow is stable or not. In this work, the temporal and spatial frameworks are evaluated. Studies addressing the temporal stability analysis of two-phase flow as Couette or Poiseuille plane can be found in the literature (Valluri et al., 2008; Sahu et al., 2007; Cao et al., 2004; Boomkamp and Miesen, 1997; Kuru et al., 1995). However, studies related to spatial analysis, due to the higher computational effort, have attracted little attention, being an open field for research.

This work presents 2D numerical simulations using VOF method to study the local Linear Stability Theory LST, in temporal and spatial frames, of a parallel stratified two-phase flow in a plane channel analogous to water-oil case evaluated by Gada and Sharma (2012) and Rodríguez (2015). Results are compared with an Orr-Sommerfeld-like approach for two-separated phases.

2. MODEL FORMULATION

Stability analysis in stratified two-phase flows is investigated by introducing controlled perturbations at interface of a fully developed base flow. The evolution, in time and space, of the interfacial waves introduced, allowing to monitor parameters that describe the wave stability. Both fluids are considered as incompressible, and the fully developed base flow is determined numerically. Figure 1 illustrates the stratified flow between two parallel planes with cross section height H. The temporal case investigated is outlined in Fig. 1a, where the length of the domain L is equal to wavelength λ of a particular mode studied, and periodic conditions between input and output are specified. In Fig. 1b, the spatial case considers a length domain L larger than the temporal case, with a fully developed flow prescribed at the inlet, and with constant pressure imposed at the outlet. No-slip conditions at top and bottom walls complement the model formulation. Local linear stability analysis consider perturbations q' of the form,

$$q'(x,y,t) \sim \hat{q}(y)\exp\left[i(\alpha x - \omega t)\right] \tag{1}$$

where the amplitude function $\hat{q}$, represents any variable of flow field (normal velocity, pressure, etc); α and ω are the wavenumber and circular frequency, respectively. The nature of these terms (real or complex), depend on the framework considered.

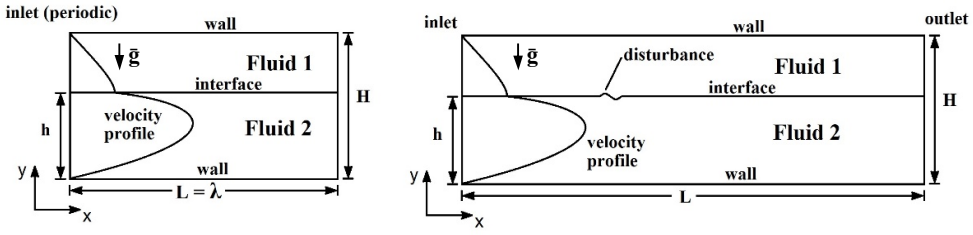

(a) Temporal framework (b) Spatial framework

Figure 1. Flow configuration.

2.1 Mathematical model

To determine the flow field, the conservation of mass and momentum are solved considering only one set of conservation equations, assuming a variable property fluid, corresponding to each phase. The VOF method (Hirt and Nichols, 1981) was selected to determine the region occupied by each phase. The VOF method introduces a marker function or volume fraction β_k that has a unit value in the region of domain occupied by one of fluids and zero in the region occupied by the other. So, the volume fraction of each phase must obey the following relation,

$$\sum_{k=1}^{2} \beta_k = 1. \tag{2}$$

The continuity equation is

$$\frac{\partial \rho}{\partial t} + \nabla \bullet (\rho \mathbf{V}) = 0 \tag{3}$$

where **V** represents the velocity vector. To take into account the pressure jump at the interface, a forcing term proportional to the surface tension σ is include at the momentum equation, only at the interface, resulting in the following momentum equation

$$\frac{\partial}{\partial t}(\rho \mathbf{V}) + \nabla \bullet (\rho\ \mathbf{V}\mathbf{V}) = -\nabla p + \mathbf{f} + \bar{\nabla} \bullet \left[\mu\left(\nabla \mathbf{V} + \nabla \mathbf{V}^T\right) - \frac{2}{3}\mu \nabla \bullet \mathbf{V}\underline{\underline{\mathbf{I}}}\right] + \sigma \kappa \delta(n)\mathbf{n} \tag{4}$$

where p is the pressure, **f** is a body force acting on the fluids by unit of volume**, I** is identity tensor, κ and $\delta(n)$ are, respectively, the curvature and a delta function of the interface and **n** is the normal vector to the interface, and σ is the surface tension.

The interface curvature κ, the normal vector to interface $\mathbf{n}$ and the volume fraction function β_k can be related by

$$\kappa = \nabla \bullet \mathbf{n} \quad , \quad \mathbf{n}_k = \nabla \beta_k \quad , \quad \kappa = \nabla \bullet \frac{\nabla \beta_k}{|\nabla \beta_k|}. \tag{5}$$

Properties of each fluid, such as density ρ_k and viscosity μ_k were considered constant, and were obtained with the following relation:

$$\rho = \sum_{k=1}^{2} \beta_k \rho_k \quad , \quad \mu = \sum_{k=1}^{2} \beta_k \mu_k . \tag{6}$$

The volume fraction of one phase, in the absence of mass transfer, can be determined from the phase *k* mass conservation equation as

$$\frac{\partial (\rho_k \ \beta_k)}{\partial t} + \nabla \bullet (\rho_k \ \beta_k \ \mathbf{V}) = 0. \tag{7}$$

The velocity vector, pressure, spatial coordinates and time can become dimensionless as employed by Rodríguez (2015) as

$$\mathbf{U}^* = \frac{\mathbf{V}}{U_m} \quad , \quad p^* = \frac{p}{\rho_1 U_m^2} \quad , \quad \mathbf{x}^* = \frac{\mathbf{x}}{H} \quad , \quad t^* = \frac{t\, U_m}{H} \tag{8}$$

where ρ_1 is the density of fluid 1 and U_m is a mixture velocity, which is equal to the sum of phase 1 and phase 2 superficial velocities, $U_m = U_{s1} + U_{s2}$. Superficial velocities are defined as the ratio of the phase *k* volumetric flow rate $\dot{\forall}_k$ by the flow cross section area *A*, $U_{sk} = \dot{\forall}_k / A$. Thus, the fully developed plane flow field is governed by the properties ratio, Reynolds *Re*, Weber *We* and Froude *Fr* numbers:

$$\chi = \frac{\rho_2}{\rho_1} \quad , \quad \eta = \frac{\mu_2}{\mu_1} \quad , \quad Re = \frac{\rho_1 U_m H}{\mu_1} \quad , \quad We = \frac{\rho_1 U_m^2 H}{\sigma} \quad \text{and} \quad Fr = \frac{U_m}{\sqrt{gH}}, \tag{9}$$

where *g* is the acceleration of gravity.

In the present study, for both temporal and spatial frame, a disturbance in form of sinusoidal wave is introduced at interface of the fluids as a body force in the *y*-momentum equation. The equation to define the body force in the temporal frame is

$$f_y = A \sin(\alpha x) \ (1 - \beta_1) \ \beta_1 \ \ \delta(t_i) \tag{10}$$

where *A* is the amplitude of the body force, whose value is determined based on the order required for the initial interface amplitude. The δ-function guarantees that the disturbance is applied only at the initial time instant t_i. α is the wavenumber correspondent to fundamental mode studied. In this case, the disturbance has a wavelength ($\lambda = 2\pi/\alpha$) equal to the domain L, as indicated above.

Form the spatial frame, the source term is

$$f_y = A \sin(\omega_r \ t) \ (1 - \beta_1) \ \beta_1 \qquad \text{at} \quad 4\text{H} \leq \text{x} \leq 4.5\text{H} \tag{11}$$

where *A* is the amplitude defined similarly to the temporal case, and ω_r is the circular frequency correspondent to fundamental mode. In this case, the disturbance is introduced continuously in time and it is applied at a particular position far from the inlet equal to 4H, where H is the height of the channel. A constant wavelength of 0.5H is used for the disturbance that is superimposed to the fully developed base flow.

2.2 Linear Stability Problem

The standard method of normal modes is used here to obtain an equation which relates frequencies and wavenumbers, that is so called dispersion equation. Depending on temporal or spatial analysis, one can prescribe a real frequency and obtain a complex wavenumber or one can prescribe a real wavenumber to obtain a complex frequency. For this case, the solution delivers a complete eigenspectrum of modal solutions. The imaginary part of the complex eigenvalue (frequency

or wavenumber, depending on analysis) determines the asymptotic amplitude growth or decay of a particular mode, indicating if the flow is stable or not.

For base flows composed of different and immiscible phases, the usual approach (Kuru et al., 1995; Boomkamp and Miesen, 1997) is to discretize the Orr-Sommerfeld equation for each phase individually and couple the two systems of equations through interfacial conditions, imposing the continuity in velocity and tangential stresses, plus the balance between normal stresses and the interfacial tension. In this paper the same strategy is adopted. The Orr-Sommerfeld (O-S) equations are discretized using 5th order finite differences and the resulting matrix eigenvalue problem is solved using the standard QZ algorithm.

3. NUMERICAL METHOD

Determination of the two-phase flow with the VOF method (Hirt and Nichols, 1981) can be performed using classical procedures for monophasic flow solution. In this study, we selected commercial software ANSYS FLUENT®. This software is based on the finite volume method, where the computational domain is divided into control volumes and the conservation equations are integrated into each volume. To evaluate the convective and diffusive fluxes of the momentum equation, the *Power-Law* scheme was selected (Patankar, 1980). The volume fraction was discretized implicitly with the *compressive scheme* of Fluent (2013), which is a high order reconstruction scheme based on a slope limiter, like a TVD scheme (Prosperetti e Tryggvason, 2007), that allows to obtain sharp interfaces. The pressure-velocity coupling was handled with the *Coupled scheme* of Fluent (2013), which is achieved through an implicit discretization of pressure gradient terms in the momentum equations, and an implicit discretization of the face mass flux, including the Rhie-Chow pressure dissipation terms. The system of algebraic equation was solved using the Gauss-Seidel line-by-line algorithm, coupled with the additive multigrid method (Hutchinson e Raithby, 1986). For the time integration, an implicit 2nd order algorithm was applied.

3.1 Post-processing of numerical simulations

A simple method is used to obtain the amplification rate and phase velocity of the numerical simulation. In the temporal case, the amplitude growth of an interfacial wave contained in the periodic domain is estimated by the amplitude mainstream wave at each time step. This results in a temporal variation of maximum amplitudes that in logarithmic scale, the slope of the wave provides directly the temporal growth rate. Phase velocity is obtained by the spatial displacement of these wave peaks for each time step.

In the spatial case, an envelope of amplitudes is obtained from the spatial evolution of an interfacial wave along the streamwise direction. In this case we determine a region that excludes the perturbation zone and the domain outlet, where we obtain the spatial evolution described. Thus, the growth rate of the waves is obtained as a straight slope in the amplitude evolution. The phase velocity is obtained by tracking the peaks of the waves and their coordinate *x*, similar to the temporal case.

4. RESULTS

To analyse the temporal and spatial instability of the plane channel flow, the following parameters were defined:

$$\chi = 1.218 \quad , \quad \eta = 0.1874 \quad , \quad Re = 241.5 \quad , \quad We = 9.22 \quad \text{and} \quad Fr = 3.017 \tag{12}$$

According to the prescribed flow parameters, a fully developed base flow condition was achieved when both the maximum velocity ($U^*_{\mathbf{max}}$) reached a value of 1.743 and the liquid height (h^*) reached 0.558. These non-dimensional values were given previously in the works of Gada and Sharma (2012) and Rodríguez (2015). In the present work, a steady state simulation was used to calculate of the base flow. Thus, developed base flow was used as the initial condition for the transient simulation in temporal case (periodic boundary conditions) and as initial and inlet boundary condition in the spatial case (non-periodic boundary conditions).

Since the transient simulation in temporal case was carried out using periodic boundary conditions, the computational domain was restricted to only few diameters in length, hence the simulation cost was considerably reduced. Two scenarios were investigated using this approach. In the first scenario, it was observed the evolution of disturbances introduced in the flow by the numerical noise inherent to the simulation. In the second scenario, disturbances having amplitudes higher than the numerical noise were introduced artificially in the flow. In this last case, the disturbance wavelength was selected in order to enable for a direct comparison with linear stability calculations. Three different mesh resolutions were tested in all cases (70×210, 70×315 and 70×420) for the domain $H^*\times L^*$, where H^* and L^* are the non-dimensional height and length channel, respectively. Previous simulations, not included here, showed that the mesh refinement in vertical direction did not improve the results for a number of elements higher than 70. In the present paper, the more representative results are shown with indication of the mesh used. In both scenarios the amplification of the disturbances was analysed for different mesh resolutions. Therefore, the effect of mesh refinements was addressed at reduced computational cost.

Figure 2 presents the temporal evolution of numerical noise for a streamwise domain L^*=3 and a mesh resolution equals to 70×315. According to the results shown in the figure, the initial amplitude of numerical noise is in the order of 10^{-7}. Iso-contours of wall normal velocity fluctuations are also displayed in the figure in order to illustrate the disturbance characteristics at different time instants. As a reference the interface is also displayed in the graphs. It can be observed that initially, the wall normal velocity is, basically, composed of disturbances with very small wavelengths. At this instant the oscillation of the interface is also very small. After the initial transient, disturbances having larger wavelengths are amplified and become more prominent. At intermediate time instants, the interface oscillation remains very small but the iso-contours of wall normal velocity display a periodic spatial behaviour. It is conjectured here, that such pattern is related with one of the most unstable modes according to the linear stability. In the last half of the simulation time, there is a noticeable change in both iso-contours of velocity and interface height. At this stage nonlinear effects might be present causing a rapid amplification of the disturbances. In the end of the simulation, the amplitudes display a clear saturation and the interfaces show a clearly non sinusoidal pattern. This is an indicative of fully non-linear regime and this regime will be not addressed in this work.

According to the results of Fig. 2, several stages can be observed in the evolution of non-controlled disturbances. For different time instants, disturbances having distinct wavelengths were the most prominent ones. It was not found a time instant when amplitude of the predominant mode was far higher than the amplitude of non-dominant modes. Therefore, the growth of the disturbances could not be linked to any individual mode.

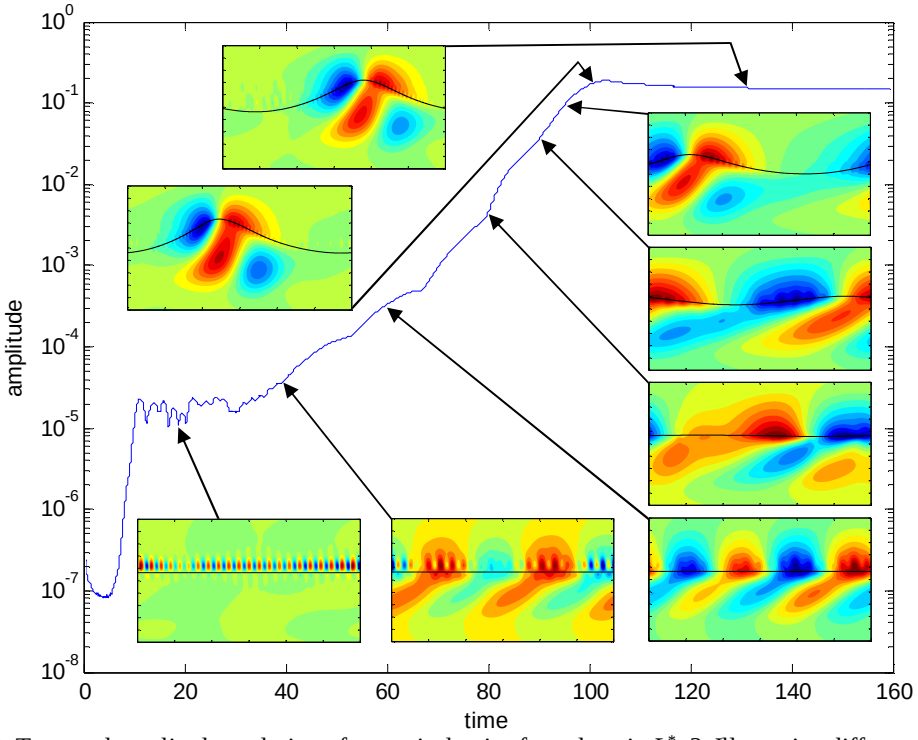

Figure 2. Temporal amplitude evolution of numerical noise for a domain L^*=3. Illustrative different instants to normal velocity contour (at local instant values) are shown with interface reference.

During the initial transient displayed in the graph of Fig. 2, a rapid amplification of the disturbances was observed. This behaviour can be regarded as a transient algebraic growth (Schmid and Henningson, 2001). The transient growth was captured because the simulation solves the full governing equations.

For a direct comparison between numerical simulations and LST calculations, waves with a well-defined wavelength were introduced in the flow, at the beginning of simulation, and their evolution in time was analysed. The wavelength of the excited waves was chosen to correspond to the channel length. Figure 3 shows a comparison between simulation and LST for the case with a channel length L^* equals to 1.5. Iso-contours of wall normal velocity are displayed. As can be observed, the results from the simulation are in qualitative agreement with the eigenfunctions given by LST. The results show that both amplitudes and phases could be well captured by the simulations.

Amplitude evolution of waves in cases of controlled disturbances is shown in Fig. 4a for a non-dimensional channel length of 3. In the case of Fig. 4a an intermediate mesh grid was used (70×315). In the first time steps close to the instant when the disturbances were introduced in the flow a strong transient algebraic growth appears and predominates over the exponential effect. Afterwards, exponential growth of fundamental mode dominates. Thus, the exponential growth of the mode corresponding to the excited disturbance wavelength could be captured and the amplification rates were well resolved. This enables a further comparison with O-S calculations. The amplitude curve of Fig. 4a displays an earlier

saturation of wave growth in comparison with non-disturbed case. Similar behaviour is observed by other authors (Valluri et al., 2008; Cao et al., 2004) for other conditions studied. However, it can be clearly seen here that amplitude levels at the saturation were rather similar in both disturbed and non-disturbed cases. The results suggest that saturation occur only when oscillations at the interface reach few tenths of the channel height. In addition, the same tendency of exponential growth observed for small disturbances holds for stages very close to saturation.

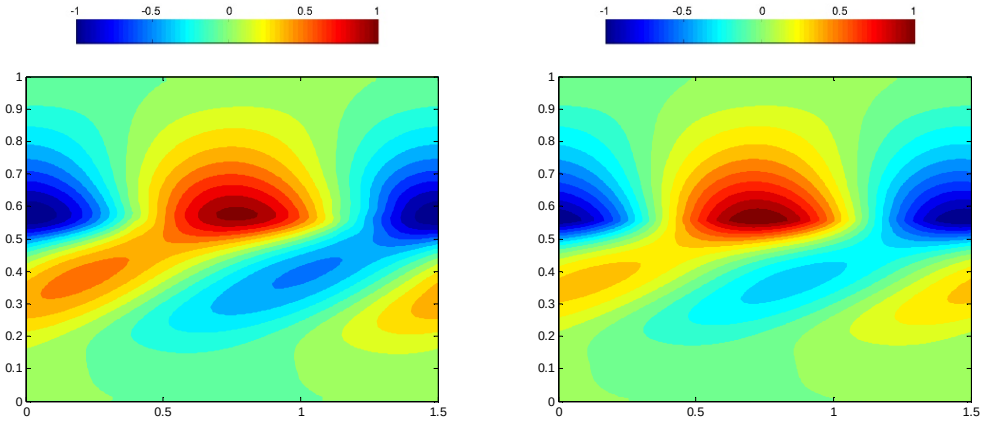

(a) Numerical simulations (b) O-S approach

Figure 3. Qualitative comparison of temporal fundamental mode for L^*=1.5.

In Fig. 4b, the linear growth of the disturbance amplitude are depicted for three different mesh resolutions. It can be clearly seen that the slope of the curves approach the values predicted by linear stability analyses with the grid refinement. Results obtained with the finest mesh resolution used in the simulations were compared against O-S calculations in Tab.1. In the table are displayed values of amplification rate ω_i and phase velocity $c_p=\omega_r/\alpha$. Cases with different domains and hence disturbance wavelengths were compared. A good agreement between theory and simulations was observed. The phase velocity for the domains L^*=1.5 and L^*=3 have a difference from the O-S solution of about 0.3%, and for L^*=4 the difference is about 1%. For the amplification factor, the comparison presents slightly larger differences. For the domain L^*=1.5 and L^*=3 the difference is about 7%, and a smaller difference (4%) was obtained for L^*=4.

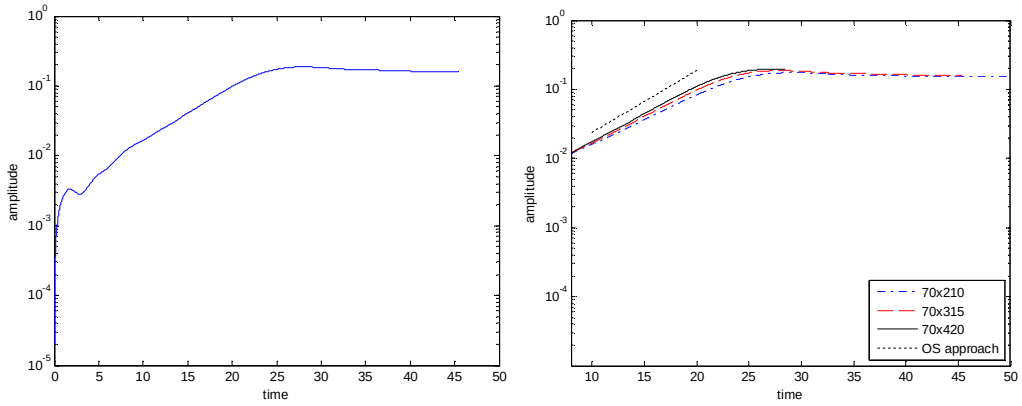

(a) Complete behavior captured by numerical simulation

(b) Comparative amplification rates to to different mesh resolution

Figure 4. Disturbance amplitude evolution in time for L^*=3. To allow for a better visualization, the initial transient algebraic growth is not shown in (b).

Table 1. Temporal stability analysis results (mesh resolution $H^*\times L^*$=70x420). Comparison with O-S calculations.

Case	$L^*=\lambda$	c_p	c_p (O-S)	ω_i	ω_i (O-S)
1	1.5	1.533	1.537	0.102	0.109
2	3	1.396	1.399	0.192	0.206
3	4	1.383	1.367	0.202	0.194

In spatial case, the domain is rather large in comparison with the temporal case domain, therefore fewer cases were simulated due to the high computational cost. The mesh employed was 70×6300 in a domain with length L^*=30 which is equivalent to 1.5 times more cells than those of the temporal reference case with the finest grid (L^*=3, 70×420). In the spatial analysis, a continuous sinusoidal disturbance with a frequency ω_r and a wavelength of $0.5H^*$, was superimposed to the fully developed base flow. The disturbance was applied to the flow close to the interface at a distance of $4H^*$ from the inlet. The excited disturbances evolved convectively along the streamwise direction until reaching the outlet. Figure 5 shows a snapshot of wall normal velocity fluctuations along the simulation domains. In this case, the non-dimensional disturbance frequency was set to ω_r=2.5. At the domain outlet, some qualitatively differences are generated due to imposing constant pressure as outlet condition. Although the outlet condition is expected to have little effect on interface growth, this region was not considered for post processing of data obtained from the simulation.

The evolution of waves along the streamwise direction was also studied for a non-dimensional frequency of 5. Table 2 shows the results from the present simulation and O-S calculations. For this last one, Gaster's transformation (Gaster, 1962) was used to convert theoretical amplification rates obtained from temporal instability analysis into spatial growth rates. A good agreement was obtained for phase velocity c_p and some differences were obtained in the amplification rate α_i. The phase velocity for the case with frequency ω_r=2.5 presented a difference of about 0.4%, and for the case with ω_r=5 the difference is about 1%. These differences are comparable to the ones obtained for phase velocity in the temporal framework. Moreover, the difference between the models for the amplification factor is about 7% for the case with frequency ω_r=2.5. Substantial difference was obtained for the case with larger frequency ω_r=5. Apparently, this difference might be related with the bad choice of parameters used for the excitation of the disturbances. The extent of region where the disturbances were excited was rather short in comparison to the wavelength of the corresponding O-S mode. As can be seen in Fig. 5 the wavelength of the most amplified disturbance is rather longer than $0.5H^*$. Thus, disturbances in other wavelengths than that corresponding with the O-S mode were introduced in the flow. The scenario resembles the non-disturbed temporal case, that was depicted in Fig. 2. Thus, the accuracy in the estimation of the amplification rates could be affected by the presence of disturbances with several different wavelengths. In addition, it is important to indicate that the outlet boundary condition and indirect method used (Gaster's transformation) to obtain spatial results can also influence on this difference. Nevertheless, another and maybe more important factor to the observed differences can be associated with numerical diffusion of VOF method (Prosperetti e Tryggvason, 2007). The inherent artificial viscosity could be attenuating the grown of interfacial waves. This issue motives strong research to find the best efficient technique in numerical simulation to model the two-phase flow instability that can compare theoretical results of rigorous models.

(a) Numerical simulations

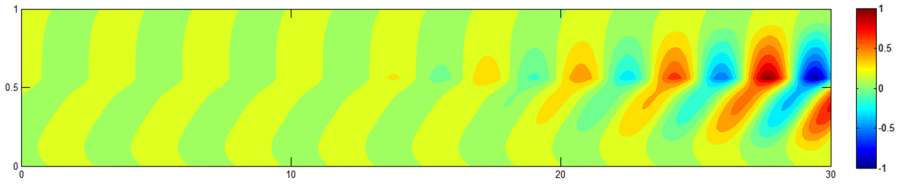

(b) O-S approach

Figure 5. Qualitative comparison of spatial instability for ω_r=2.5.

Table 2. Spatial stability results (mesh resolution 70×6300 in domain $L^*=L/H=30$).

Case	ω_r	c_p	c_p (O-S)	α_i	α_i (O-S)
1	2.5	1.375	1.380	-0.127	-0.136
2	5	1.472	1.489	-0.075	-0.108

5. FINAL REMARKS

Temporal non-disturbed cases allow us to determine the order of the numerical error of simulations as consequence of spatial and temporal discretization schemes used. Values on the order of 10^{-7} show that the schemes used are valid for the study of introduced perturbations with amplitudes of at least 10^{-5}.

The studied cases are linearly unstable. Besides, spatial analysis let us add to the previous conclusion that the flow is convectively unstable, too. The evaluated cases show good agreement with theoretical results, showing that the numerical tool used can be adequately to study stability of different cases in other configuration like circular pipe flow or in general 3D settings.

The numerical simulation proves to be an adequate tool to study the linear stability of the two-phase flow. The VOF method delivers results whose error is acceptable allowing to evaluate the flow stability taking into account that the controlled disturbances of very small amplitude always are much larger than the simulation noise.

6. ACKNOWLEDGEMENTS

The authors would like to acknowledge the supported granted during the development of this work by the Brazilian Government agencies: CNPq, CAPES and ANP.

7. REFERENCES

ANSYS Fluent 15.0, Theory Guide, 2013, Ansys Inc., Canonsburg, PA, U.S.A.

Barnea, D. and Taitel, Y., 1993. “Kelvin-Helmholtz Stability Criteria Stratified Flow: Viscous versus Non-Viscous (Invicid) Approaches”. International Journal of Multiphase Flow, Vol. 19, No. 4, pp. 639-649.

Boomkamp, P.A.M. and Miesen, R.H.M., 1997. “Classification of instabilities in parallel two-phase flow”. International Journal of Multiphase Flow, Vol. 22, No. Suppl., pp. 67-88.

Cao, Q., Sarkar, K. and Prasad, A.K., 2004. “Direct numerical simulations of two-layer viscosity-stratified flow”. International Journal of Multiphase Flow, Vol. 30, pp. 1485-1508.

Eduardo, T.H.T., de Paula, I.B. and Nieckele, A.O., 2015. “Transition from stratified to slug flow regime in the presence of controlled perturbations on the liquid level”. IV Journeys in Multiphase Flows (JEM2015).

Gada, V.H. and Sharma, A., 2012. “Analytical and level-set method based numerically on oil-water smooth/wavy stratified-flow in an inclined plane-channel”. International Journal of Multiphase Flow, Vol. 38, pp. 99-117.

Gaster, M., 1962. “A note on the relation between temporally-increasing and spatially-increasing disturbances in hydrodynamic stability”. Journal of Fluid Mechanics, Vol. 14, pp. 222-224.

Guo, L., Li, G. and Chen, X., 2002. “A linear and non-linear analysis on interfacial instability of gas–liquid two-phase flow through a circular pipe”. International Journal of Heat and Mass Transfer, Vol. 45, pp. 1525-1534.

Hirt, C. and Nichols, B., 1981. “Volume of Fluid (VOF) Method for the Dynamics of Free Boundaries”. Journal of computational physics, Vol. 39, pp. 201-225.

Hutchinson, B.R. and Raithby, G.D., 1986. “A Multigrid Method Based on the Additive Correction Strategy”. Numerical Heat Transfer, Vol. 9, pp. 511-537.

Ishii, M. and Hibiki, T., 2011. “Thermo-Fluid Dynamics of Two-Phase Flow”. Second Edition, Springer, New York.

Kuru, W.C., Sangalli, M., Uphold, D.D. and McCready, M.J., 1995. “Linear Stability of Stratified Channel Flow”. International Journal of Multiphase Flow, Vol. 21, No. 5, pp. 733-753.

Lin, P.Y. and Hanratty, T.J., 1986. "Prediction of the Initiation of Slugs whit Linear Stability Theory". International Journal of Multiphase Flow, Vol. 12, No. 1, pp. 79-98.

Patankar, S.V., 1980. “Numerical Heat Transfer and Fluid Flow”. McGraw-Hill Book Company.

Prosperetti, A. and Tryggvason, G., 2007. “Computational Methods for Multiphase Flow”. Cambridge University Press.

Rodríguez, D., 2015. “A novel modeling method for the interfacial instability of inmicible fluids along ducts”. 23rd ABCM Int. Congress of Mechanical Engineering (COBEM 2015).

Sahu, K.C., Valluri, P., Spelt, P.D.M. and Matar, O.K., 2007. “Linear instability of pressure-driven channel flow of a Newtonian and a Herschel-Bulkley fluid”. Physics of Fluids, Vol. 19, pp. 122101(1-11).

Salhi, Y., Si-Ahmed, E., Legrand, J. and Degrez, G., 2010. “Stability analysis of inclined stratified two-phase gas–liquid flow”. Nuclear Engineering and Design, Vol. 240, pp. 1083-1096.

Schmid, P.J. and Henningson, D.S., 2001. “Stability and Transition in Shear Flows”. Springer-Verlag New York, Inc.

Taitel, Y. and Dukler, A.E., 1976. “Model for predicting flow Regime transitions in horizontal and near horizontal gas-liquid flow”. AIChE Journal, Vol. 22, No. 1, pp. 47-55.

Valluri, P., Ó Náraigh, L., Ding, H. and Spelt, P.D.M., 2010. “Linear and nonlinear spatio-temporal instability in laminar two-layer flows”. Journal of Fluid Mechanics, Vol. 656, pp. 458-480.

Valluri, P., Spelt, P.D.M., Lawrence, C.J. and Hewitt, G.F., 2008. “Numerical simulation of the onset of slug initiation in laminar horizontal channel flow”. International Journal of Multiphase Flow, Vol. 34, pp. 206-225.

Yiantsios, S.G. and Higgins, B.G., 1988. “Linear stability of plane Poiseuille flow of two superposed fluids”. Physics of Fluids, Vol. 31, No. 11, pp. 3225-3238.

8. RESPONSIBILITY NOTICE

The authors are the only responsible for the printed material included in this paper.